

EQUILIBRIUM, KINETIC, AND THERMODYNAMIC STUDIES OF LEAD (II) BIOSORPTION ON SESAME LEAF

Li-e Liu,^{a, b} Jindun Liu,^{a,*} Hongping Li,^b Haoqin Zhang,^a Jie Liu,^b and Hongquan Zhang^b

Sesame leaf, an agricultural solid waste, was used as low cost adsorbent for removal of Pb(II) from aqueous solution in batch mode. The biosorbent was characterized by thermo-gravimetric analysis and Fourier transform infrared spectroscopy. The influences of phase contact time, solution pH, adsorbent dosage, and initial concentrations were investigated to optimize the conditions for maximum adsorption. The experimental data were analyzed by Langmuir, Freundlich, and Koble-Corrigan isotherm models. The Koble-Corrigan and Langmuir isotherms best represented the measured biosorption data. According to an evaluation using the Langmuir equation, the adsorption capacity of the biosorbent was found to be 279.86 mg g⁻¹, which was higher or comparable to the adsorption capacity of various adsorbents reported in the literature. The kinetics of adsorption of Pb(II) was evaluated by pseudo-first order, pseudo-second order, and intra-particle diffusion kinetic models. The experimental data fitted very well with the pseudo-second order kinetic model. The intra-particle diffusion model is not a dominant rate controlling mechanism in the sorption of Pb(II). Thermodynamic analysis showed that the adsorption was a spontaneous and endothermic process. The results indicated that sesame leaf can be used as an effective biosorbent for Pb(II) removal from aqueous solutions.

Keywords: Biosorption; Lead; Sesame leaf; Kinetics; Isotherm; Thermodynamics

Contact information: a: School of Chemical Engineering and Energy, Zhengzhou University, Kexue Road 100#, Zhengzhou, Henan 450001, PR China; b: School of Public Health, Zhengzhou University, Kexue Road 100#, Zhengzhou, Henan 450001, PR China

*Corresponding author: liujindun@zzu.edu.cn (J.D. Liu)

INTRODUCTION

Among the different heavy metals, lead is one of the most dangerous contaminants released into the natural waters from various industrial activities such as mining and melting of metallic ferrous ores, oil refining, municipal wastes, paint and pigment production, and battery manufacturing (Axtell *et al.* 2003). When the human body is exposed to lead, it can enter through inhalation or dermal contact. It tends to accumulate in living tissues such as bone, brain, kidney, and muscles, and it may cause many significant diseases such as anemia, nephropathy, blood and brain disorders, and ultimately cause death (Kazi *et al.* 2008; Afridi *et al.* 2006). Due to toxic effects of lead ions, the World Health Organization (WHO) established 3 to 10 µg L⁻¹ as the maximum permissible limits for lead in drinking water (dos Santos *et al.* 2011). However, the actual concentration of lead in wastewater can be as high as several hundred micrograms per

liter. So, the removal of lead from wastewaters before its release to unpolluted natural water bodies is important in terms of protection of public health and the environment.

In recent decades, various techniques have been used for reducing the levels of heavy metals in wastewater, including chemical coagulation, adsorption, reverse osmosis, electrolysis, ion exchange, and membrane separation (Chen *et al.* 2010). Among these methods, using the adsorption technique for the removal of some heavy metals from solutions has recently attracted widespread attention (Mudhoo *et al.* 2011). Adsorption has become one of the most effective methods (Kul and Koyuncu 2010; Astier *et al.* 2012). Low-cost adsorption methods have been researched for the removal of heavy metals from waste water from the standpoint of eco-friendly, effectiveness, and economic considerations. A variety of non-conventional materials, such as de-oiled allspice husk (Cruz-Olivares *et al.* 2010), green algae (Gupta and Rastogi 2008), mango peel (Iqbal *et al.* 2009), grape stalk (Martinez *et al.* 2006), *Phaseolus vulgaris* L (Ozcan *et al.* 2009), mushrooms (Vimala and Das 2009), Douglas fir (Astier *et al.* 2012), rose (Javed *et al.* 2007), Pang Da Hai (Liu *et al.* 2006), *Ficus religiosa* leaves (Qaiser *et al.* 2009), and pine bark (Mihailescu Amalinei *et al.* 2012) have been studied for their ability to remove heavy metals.

Sesame is extensively cultured, usually as a source of oil. The production and use of sesame oil have been established in China for more than 2000 years. Sesame oil production has been identified with the inhabitants of this area from economic, social, and cultural standpoints. Furthermore, sesame oil constitutes the main source of nutritional fats and is a very valuable product for exportation. Sesame leaf is an abundant agricultural by-product. It is arbitrarily discarded, which is not only wasteful but also pollutes the environment. Like other plant materials, sesame leaf contains plenty of floristic fiber made of cellulose, hemi-cellulose, and lignin, which suggests that it may be a suitable candidate as an economical and potential biosorbent (Allouch *et al.* 2011).

Thus, the objective of present study was to work toward the application of a novel biosorbent for heavy metal adsorption. The effects of various experimental parameters on the adsorption of Pb(II) were also investigated.

EXPERIMENTAL

Preparation and Characterization of Sesame leaf

Sesame leaf used in this study was collected from its natural habitats located in Henan Province, China. The collected materials were first soaked and extensively washed with running water to get rid of all the dirt, and then they were washed with distilled water. The spotless sesame leaf was dried at 60 °C for 20 h in an oven, then ground into powder and sifted through a nest of sieves to get a 20 to 40 mesh size. The prepared samples were enclosed in a self-sealing plastic pocket and taken for the adsorption experiments.

The thermal behavior of sesame leaf was obtained by using a thermo-gravimetric analyzer (STA 409 PC, German). About 5.42 mg of sesame leaf were heated up to 600°C in oxidant atmosphere at 10 °C min⁻¹ temperature rate.

Fourier transform infrared spectrometry (Hitachi S-4700, Japan) was used to analyze the functional groups on the surface of sesame leaf. The spectral range was from 4000 to 400 cm^{-1} .

Preparation of Pb (II) Solution

The adsorbate Pb(II) was supplied by Zhengzhou Chemical Equipment Company. The stock solution of Pb(II) was prepared by dissolving a required amount of $\text{Pb}(\text{NO}_3)_2$ in doubly distilled water at room temperature. The experimental solutions were obtained by diluting a stock solution of Pb(II) with double distilled water to the desired concentration.

Adsorption Experiment

Adsorption studies were operated by the batch technique at different temperatures (293K, 303 K, and 313 K), respectively. In each batch biosorption experiment, 20 mg of sesame leaf powder was added to 20 mL of Pb(II) solution in the concentration range of 50 to 300 mg L^{-1} in a 100 mL flask. Then the mixture was shaken at 150 rpm using a thermostatic shaker for each predetermined time interval. The mixture of Pb(II) and sorbent was separated by centrifugation at 4000 rpm for 20 min, and the concentration of remaining Pb(II) in supernatant was analyzed by atomic absorption spectrometer (Hitachi Z-5000). The reproducibility during concentration measurements was ensured by repeating the experiments three times under identical conditions and calculating the average values. Standard deviations of experiments were found to be within $\pm 5.0\%$.

The amount of Pb (II) adsorbed onto per gram of the biosorbent (q_e) and the percentage removal efficiency (R) were calculated through the following equations,

$$q_e = \frac{V(C_0 - C_e)}{m} \quad (1)$$

$$R = \frac{C_0 - C}{C_0} \times 100\% \quad (2)$$

where q_e is the adsorption capacity of Pb(II) on adsorbent (mg g^{-1}), C_0 is the initial concentration of Pb(II) (mg L^{-1}), C_e is the equilibrium Pb(II) concentration in solution (mg L^{-1}), m is the mass of adsorbent used (g), and V is the volume of Pb(II) solution (L).

To examine the effect of pH, adsorption experiments were performed at different pH values ranging from 1.71 to 5.02, adjusted using 0.1 mol L^{-1} HCl or 0.1 mol L^{-1} NaOH at 108.63 mg L^{-1} of Pb (II) solution. For kinetic studies, three initial concentrations of Pb(II) solutions, *i.e.* 54.32, 108.63, and 224.58 mg L^{-1} , were chosen.

Adsorption equilibrium experiments were also carried out at 293, 303, and 313 K, respectively. In this group of experiments Pb(II) solutions with different initial concentration, in the range of 50 to 300 mg L^{-1} , were selected. Normally, a pH of 5.0 and a contact time of 180 min were employed as adsorption conditions unless otherwise stated.

RESULTS AND DISCUSSION

Characterization of the Absorbents

Like all vegetable biomass, sesame leaf is composed of cellulose, hemi-cellulose, and lignin. Figure 1 exhibits the curves for TG and DTG for sesame leaf in the temperature range of 30 to 600 °C in oxidizing atmosphere.

The overall mass loss during thermo-gravimetric analysis can be divided into steps related to moisture, hemi-cellulose, cellulose, and lignin. Thus, as one can see, the

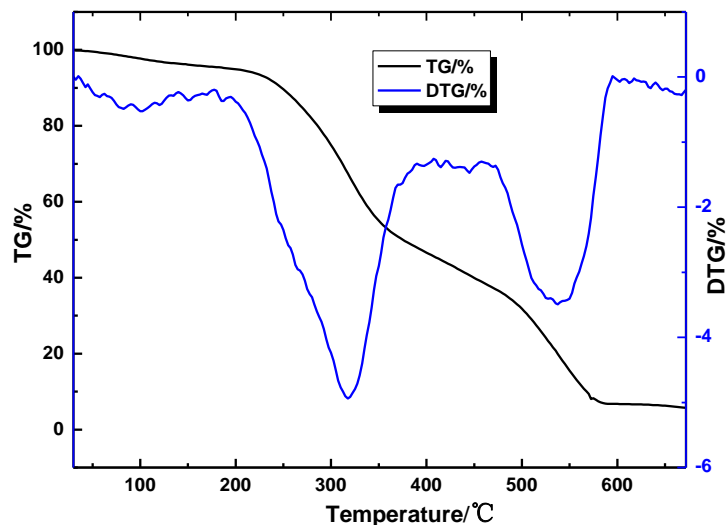


Fig. 1. Curves of thermo-gravimetric analysis (TG and DTG) of native sesame leaf

first stage of the weight loss (4.49%) can be attributed to the evaporation of physically absorbed water, structural water, and also perhaps due to the elimination of some side groups by heating the sesame leaf up to 180 °C. From 180 to 213 °C, mass loss was slight. Afterwards, the second stage of pyrolysis occurred when the temperature was varied from 213 to 430 °C. In this stage, almost all of the weight loss (53.33%) was observed with the maximum decomposition rate at 317 °C. The behavior of the pyrolysis curve at this temperature indicates hemi-cellulose and cellulose decomposition (Jayaramudu *et al.* 2011; Han *et al.* 2010). Lignin decomposition was evident in the 430 to 580 °C range (mass loss 36.50%), thus indicating that this structure was thermally more stable than hemi-cellulose and cellulose. Finally, no mass loss was detected when the temperature was increased further to 600 °C. This result indicates the presence of oxides (mainly those of aluminium and silicon), which are stable at higher temperatures.

Fourier transform infrared spectroscopy (FTIR) is often used to examine characteristic functional groups that make the adsorption behavior possible. The FTIR of sesame leaf before adsorption of Pb(II) is shown in Fig. 2a and that of sesame leaf after adsorption is presented in Fig. 2b. As can be observed from Fig. 2a, the infrared spectrum displayed a large number of absorption peaks, which indicated the presence of different types of functional groups in the biosorbent. The broadband peak at 3412 cm^{-1} was attributed to the stretching vibration of bonded hydroxyl groups on the surface of sesame leaf. The peak at 2925 cm^{-1} was assigned to the asymmetrical stretching vibration of

$-\text{CH}_3$. The symmetrical stretching vibration of $-\text{CH}_2$ gave rise to the peak at 2854 cm^{-1} . The strong band located at 1638 cm^{-1} is characteristic of stretching vibration of CO from carboxylic acid in the presence of intermolecular hydrogen bonding (Han *et al.* 2010). The peak at 1541 cm^{-1} represented the C–C stretching of aromatic rings. The peak at 1440 cm^{-1} indicated the symmetric bending of $-\text{CH}_3$. The strong peak at 1052 cm^{-1} also could be attributed to the bending vibration of $-\text{OH}$ and stretching vibration of C–O–C in lignin structure of the sesame leaf. The peak at 1259 cm^{-1} might be from the stretching vibration of C–O in phenols. From Fig. 2b, after adsorption, the peaks of the stretch vibration of bonded hydroxyl groups and that of CO stretch vibration of carboxylic acid with intermolecular hydrogen bond were shifted from 3412 cm^{-1} and 1638 cm^{-1} to 3414 cm^{-1} and 1650 cm^{-1} , respectively.

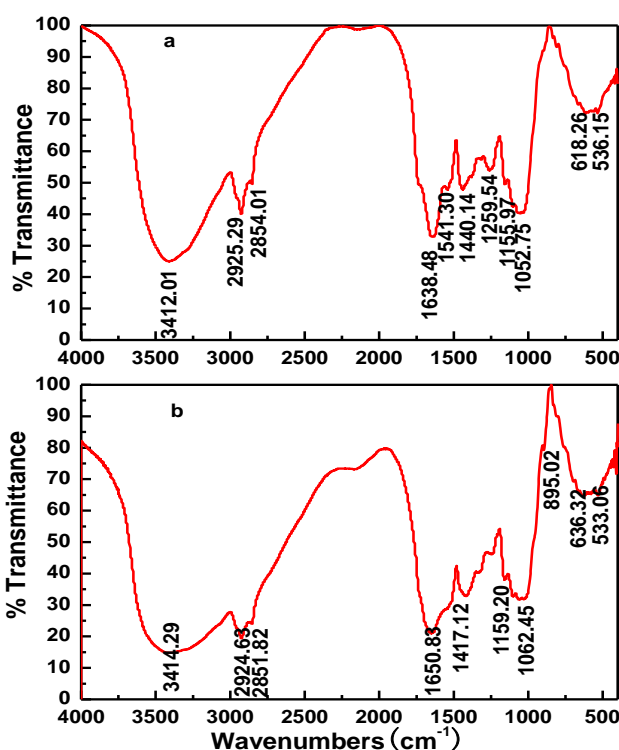


Fig. 2. Infrared spectrum of: (a) raw sesame leaf and (b) sesame leaf after adsorption of Pb (II)

The results of FTIR analysis indicated that the functional groups present in sesame leaf, such as hydroxyl and carboxyl, participated in the adsorption process for Pb(II) by surface complexation (Ngah and Hanafiah 2008; Chen *et al.* 2009).

Effect of Contact Time and Initial Pb(II) Concentrations

The adsorption equilibrium time between the adsorbate and adsorbent is important for designing batch biosorption experiments. Therefore, the adsorption of the cationic Pb(II) onto sesame leaf was studied as a function of contact time (Fig. 3a). It is evident from the figure that adsorption equilibrium was established within 180 min. And the optimum contact time was selected as 180 min for further experiments. From Fig. 3a, the adsorption rate was very fast within 30 min, and thereafter it became slower within the

range of 30 to 180 min. Finally, the adsorption capacity did not vary significantly after 180 min, and the adsorption would be in a state of dynamic equilibrium between the Pb(II) desorption and adsorption. The rapid adsorption observed during the first 30 min was probably due to the abundant availability of active sites on the sesame leaf surface, and with the gradual occupancy of these sites, the adsorption became less efficient.

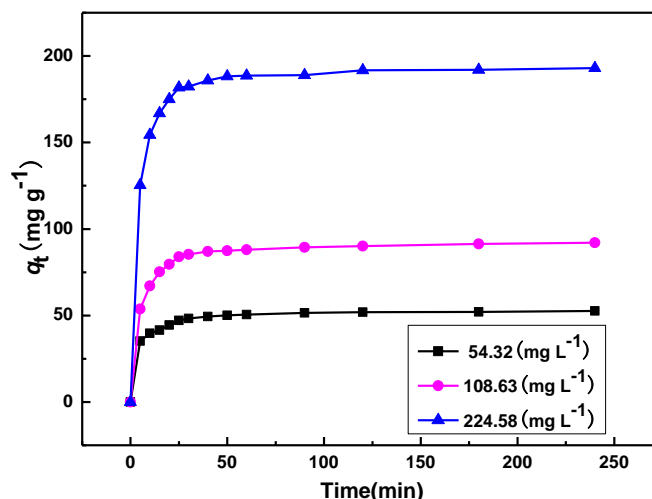


Fig. 3(a). Effect of contact time on the adsorption of Pb (II) ($C_{\text{dosage}} = 1 \text{ g L}^{-1}$; pH 5.0; $T = 303 \text{ K}$)

Figure 3a also shows that the equilibrium adsorption capacity increased from 92.00 mg g^{-1} for 108.63 mg L^{-1} to 193.89 mg g^{-1} for 224.58 mg L^{-1} . The reason is that the initial concentration provides an important driving force to overcome all mass transfer resistance of Pb(II) between the aqueous and solid phases; thus a higher initial concentration of Pb(II) will increase the biosorption amount.

The Effect of Initial pH of Pb(II) Solution

The pH of the solution is an important factor influencing heavy metal biosorption onto various adsorbents. It affects not only the surface charge of the adsorbent, but also the speciation of the heavy metal in solution. The metal cations in aqueous solution may convert to different insoluble hydrolysis products on account of pH change. This change in the form of metal species can be shown in Fig. 3b (Singh and Gadi 2012; Weng 2004).

Sorption edges as a function of pH value (1.7 to 5.0) are shown in Fig. 3c, which reveals the effect of pH on the adsorption of Pb(II) from the aqueous solution onto the sesame leaf. The uptake of lead (II) increased remarkably with the increasing pH value (1.7 to 3.3). The equilibrium uptake of Pb(II) increased from 46.5 to 103.5 mg g^{-1} with the increasing of pH from 1.7 to 3.3. The results can be explained based on the competition between Pb (II) and H_3O^+ for adsorption sites on sesame leaf. At low pH, the surface of biosorbent would also be surrounded by excess H_3O^+ which decreased the lead ions interaction with binding sites of the sesame leaf by greater repulsive forces, resulting in a low level of adsorbed Pb(II). With an increase in pH, more ligands with negative charges can be expected to be exposed, and this would attract more positively charged Pb(II) ions for binding. The effect of pH was not studied beyond pH 5.0 because of the precipitation of Pb(II) as hydroxide. Therefore, further experiments were carried out with

an initial pH value of 5.0, which confirmed that no hydroxide precipitation occurred during the process. Previous studies also have reported that the maximum biosorption efficiency for Pb(II) ion was observed at pH 5.0 (Wang *et al.* 2010; García-Rosales *et al.* 2012).

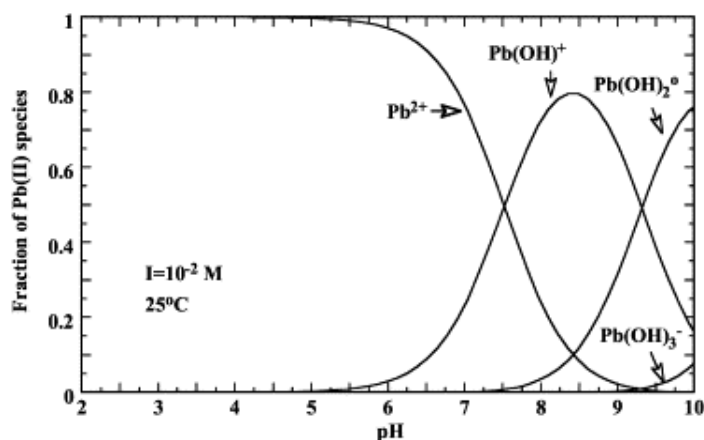


Fig. 3(b). Distribution of Pb (II) species as a function of pH

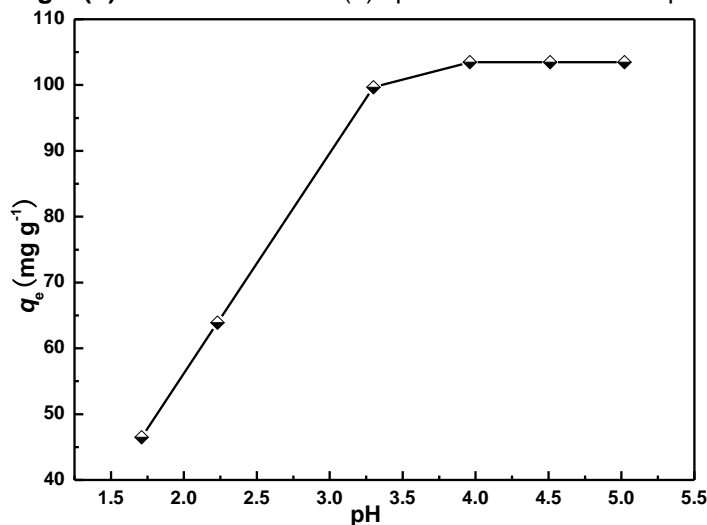


Fig. 3(c). Effect of pH on the adsorption of Pb (II) ($C_0 = 108.63 \text{ mg L}^{-1}$; $C_{\text{dosage}} = 1.0 \text{ g L}^{-1}$; $T = 303 \text{ K}$; $t = 3 \text{ h}$)

The Effect of Adsorbent Dosage

The values of the removal percentage of metal ions (R %) at different doses of sesame leaf are presented in Fig. 3d. As the sesame leaf powder concentration increased from 0.20 to 4.0 g L^{-1} , the removal efficiency of lead ions increased from 42.6% to 94.6% . This is due to the greater availability of the active sites on the adsorbent at higher concentration of the adsorbent, thus making easier penetration of the metal ions to the sorption sites (Sari *et al.* 2007). Above 1.0 g L^{-1} of adsorbent dose, the removal rate of metal ions did not remarkably increase. Therefore, an adsorbent dose of 1.0 g L^{-1} was found to be the appropriate concentration for all other batch experiments.

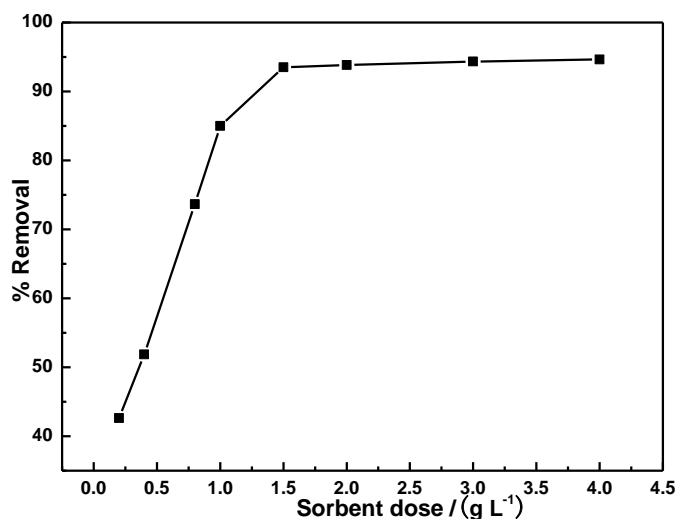


Fig. 3(d). Effect of adsorbent dose on the adsorption of Pb(II) ($C_0 = 108.63 \text{ mg L}^{-1}$; $T = 303 \text{ K}$; $t = 3 \text{ h}$)

Adsorption Isotherm

Adsorption isotherm models are commonly used to describe a relationship between concentration of lead in solution and the amount of lead adsorbed on adsorbent when both the phases are at equilibrium. It was found that the adsorption equilibrium time of Pb(II) onto sesame leaf was 180 min. Figure 4 shows plots of q_e versus of C_e for the adsorption isotherms of Pb(II) on the sesame leaf at various temperatures. Therefore, three isotherms – Langmuir, Freundlich, and Koble-Corrigan, were respectively used to analyze the equilibrium experimental data for the sorption of Pb(II) onto sesame leaf at 293, 303, and 313K. The constant parameters of the isotherm equations for these adsorption processes were calculated by non-linear regression. The isotherm data, correlation coefficients (R^2), and χ^2 values are summarized in Table 1.

The Langmuir (Langmuir 1916) isotherm model assumes the activity of every site on the surface of sorbent is identical and equivalent, and the sorbate is adsorbed homogeneously without interaction. The Langmuir equation is given as (3),

$$q_e = \frac{q_m K_L C_e}{1 + K_L C_e} \quad (3)$$

where q_e is the equilibrium adsorption capacity per unit weight adsorbent (mg g^{-1}), q_m is the theoretical maximum adsorption capacity per unit weight adsorbent (mg g^{-1}), K_L is Langmuir adsorption constant (L mg^{-1}), C_e is the equilibrium concentration of the solution (mg L^{-1}), and C_0 is maximum initial Pb(II) concentration (mg L^{-1}).

To determine whether the adsorption is favorable, a dimensionless constant, commonly known as separation factor (R_L) is defined by Webi and Chakravort (1974),

$$R_L = \frac{1}{1 + K_L C_0} \quad (4)$$

where K_L is the Langmuir isotherm constant ($L\ mg^{-1}$), and C_0 is the initial Pb(II) concentration ($mg\ L^{-1}$). The R_L value indicates whether the type of the isotherm is linear ($R_L=1$), favorable ($0 < R_L < 1$), unfavorable ($R_L > 1$), or irreversible ($R_L = 0$) (Wang *et al.* 2010).

The Freundlich isotherm (Freundlich 1906) is based on multilayer adsorption state, which means that the surface of the sorbent is heterogeneous and the adsorption is a non-uniform distribution of heat of sorption. The Freundlich isotherm model can be described as,

$$q_e = K_F C_e^{\frac{1}{n}} \quad (5)$$

where K_F and n are the Freundlich constants, K_F is the adsorption capacity of the adsorbent ($mg\ g^{-1}\ (L\ mg^{-1})^{1/n}$), and n is a constant indicative of the intensity of the adsorption.

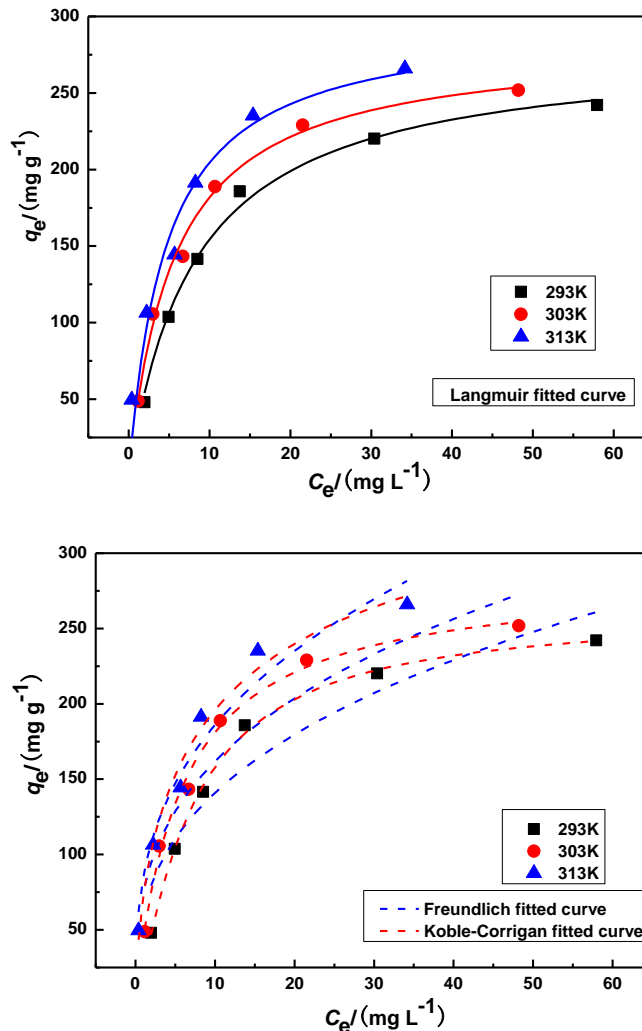


Fig. 4. The isotherms: Langmuir isotherms, Freundlich, and Koble-Corrigan isotherms

The Koble–Corrigan isotherm is a combined form of Langmuir and Freundlich isotherm models for representing the equilibrium adsorption data. The Koble–Corrigan equation can be represented as (Foo and Hameed 2010),

$$q_e = \frac{AC_e^m}{1 + BC_e^m} \quad (6)$$

where A , B , and m are the Koble–Corrigan isotherm constants, which are evaluated from the non-linear regression using a trial and error optimization.

The experimental isotherms at 293, 303, and 313K are graphically depicted in Fig. 4. A non-linear regression was used to determine the best-fitting isotherm. From Table 1 and Fig. 4, Koble-Corrigan and Langmuir isotherms were found to be suitable for adsorption with high R^2 at different temperatures. Furthermore the values of R_L from the Langmuir isotherm were between 0 and 1, and the Freundlich constant $1/n$ was smaller than 1, indicating a favorable process. The theoretical maximum adsorption capacity of sesame leaf was 279.86 mg g⁻¹ from the Langmuir isotherm at 293K; the maximum adsorption capacities q_m improved with the increase in temperature, demonstrating an endothermic process. Table 2 compares the adsorption capacity for Pb(II) to other agricultural by-products reported in the literature. The high adsorption capacity reported in this paper revealed that sesame leaf can be employed as a promising adsorbent to remove Pb(II).

Table 1. Isotherm Constants of Three Isotherm Models ($C_0 = 50\text{-}300\text{ mg L}^{-1}$; $C_{\text{dosage}} = 1.0\text{ g L}^{-1}$; $T = 293, 303, \text{ and } 313\text{K}$; $t = 3\text{h}$)

Isotherm model	constants	293K	303K	313K
Langmuir	q_e^{calc} (mg g ⁻¹)	279.86	283.01	298.76
	K_L (L mg ⁻¹)	0.123±0.011	0.179±0.018	0.216±0.056
	R_L	0.026-0.140	0.018-0.100	0.0152-0.085
	R^2	0.9943	0.9931	0.9625
	χ^2	38.77	51.22	308.86
Freundlich	K_F / [mg g ⁻¹ (L mg ⁻¹) ^{1/n}]	62.86±13.12	75.33±13.19	85.43±9.77
	1/n	0.351±0.062	0.332±0.0562	0.338±0.040
	R^2	0.9113	0.9202	0.9633
	χ^2	599.13	590.41	302.39
Koble-Corrigan	A (L ⁿ mg ¹⁻ⁿ g ⁻¹)	25.74±3.57	52.35±8.70	88.70±13.12
	B (L mg ⁻¹) ⁿ	0.099±0.012	0.183±0.026	0.22±0.066
	m	1.19±0.08	0.97±0.13	0.63±0.16
	R^2	0.9980	0.9932	0.9841
	χ^2	18.00	67.25	174.40

Table 2. Comparison of Lead Sorption Capacity of Sesame Leaf with Various Adsorbents

Adsorbent	q_e (mg g ⁻¹)	References
<i>Fontinalis antipyretica</i>	68	Martins <i>et al.</i> 2011
Oil palm empty fruit bunch	125	Haron <i>et al.</i> 2011
Formaldehyde-treated onion skins	200	Saka <i>et al.</i> 2011
Fallen <i>Cinnamomum camphora</i> leaves	73.15	Chen <i>et al.</i> 2010
Wheat bran	69.0	Bulut and Baysal 2006
Tea waste	65.0	Amarasinghe <i>et al.</i> 2007
Agro waste of black gram husk	49.97	Saeed <i>et al.</i> 2005
<i>Posidonia oceanica</i>	140	Allouche <i>et al.</i> 2011
Rose waste	156	Javed, M. A. <i>et al.</i> 2007
Sesame leaf	279.86	This study

Thermodynamic Parameters

To estimate the effect of temperature on the adsorption of Pb(II) onto sesame leaf wastes, changes in three thermodynamic parameters were evaluated: Gibbs free energy change (ΔG^0) was calculated from Equation (7),

$$\Delta G^0 = -RT \ln K \quad (7)$$

where ΔG^0 is the Gibbs free energy change (kJ mol⁻¹), R is the gas constant (8.314 J K⁻¹ mol⁻¹), T is the absolute temperature (K), and K is an equilibrium constant obtained by multiplying the Langmuir constant K_L (L mol⁻¹).

The change of enthalpy (ΔH^0) and entropy (ΔS^0) can be obtained from the slope and intercept of the Van't Hoff equation (8) of ΔG^0 versus T (Blázquez *et al.* 2011),

$$\Delta G^0 = \Delta H^0 - T\Delta S^0 \quad (8)$$

where ΔH^0 is the enthalpy change (kJ mol⁻¹) and ΔS^0 is the entropy change (kJ mol⁻¹ K⁻¹).

Values of the standard Gibbs free energy change for the adsorption process gained from Eq. (8) are listed in Table 3. The negative values of ΔG^0 at all temperatures indicate the spontaneous nature of lead biosorption onto sesame leaf. The negative value of ΔG^0 decreased with an increase in temperature, suggesting that a better adsorption is actually obtained at higher temperatures.

Table 3. Thermodynamic Parameters for the Equilibrium Sorption of Pb(II)

T (K)	293	303	313
ΔG^0 (kJ·mol ⁻¹)	-24.72	-26.51	-27.88
ΔH^0 (kJ·mol ⁻¹)		21.52	
ΔS^0 (kJ·mol ⁻¹ ·K ⁻¹)		0.158	

The standard enthalpy and entropy changes of adsorption determined from the Eq. (8) were 21.52 kJ mol⁻¹ and 0.158 kJ mol⁻¹ K⁻¹, respectively. The positive value of ΔH^0 implies an endothermic nature of adsorption. Additionally, the positive value of ΔS^0

confirmed the increased randomness at the solid-solute interface during the adsorption process, which shows the solution system tends toward stability when the adsorption of Pb(II) on the surface of adsorbent occurred according to the second law of thermodynamics.

Adsorption Kinetics

Kinetic models can be helpful to comprehend the mechanism of metal adsorption and estimate performance of the adsorbents for metal removal. In order to further determine the mechanism of Pb(II) adsorbed onto sesame leaf powder, several kinetic models were exploited to discern the controlling mechanism. They included the pseudo-first-order, pseudo-second-order, and intra-particle diffusion models. The conformity between the experimental data and the model-predicted values was expressed by coefficients of determination (R^2) and standard deviation (SD) values. The pseudo-first-order equation of Lagergren is expressed as,

$$q_t = q_e(1 - e^{-k_1 t}) \quad (9)$$

where q_e and q_t are the amount of solute adsorbed (mg g^{-1}) at equilibrium and time t (min), respectively, and k_1 is the rate constant of the pseudo-first-order adsorption (min^{-1}).

The pseudo-second-order model is based on the assumption that the rate-limiting step involves chemisorption. The equation can be written as follows,

$$q_t = \frac{k_2 q_e^2 t}{1 + k_2 q_e t} \quad (10)$$

where k_2 is the rate constant of the pseudo-second-order adsorption ($\text{mg g}^{-1} \text{min}^{-1}$). The initial adsorption rate h_0 ($\text{mg g}^{-1} \text{min}^{-1}$) at $t = 0$ is defined as follows: $h_0 = k_2 q_e^2$.

The intra-particle diffusion model proposed by Weber and Morris is given by the following equation (Weber and Morris 1963),

$$q_t = k_{id} \cdot t^{1/2} + C_i \quad (11)$$

where k_{id} is the intra-particle diffusion rate constant ($\text{mg g}^{-1} \text{min}^{-0.5}$) and C is the intercept. The value of C relates to the thickness of the boundary layer. In general, the larger C , the greater is the boundary layer effect (Kavitha and Namasivayam 2007).

Different kinetic parameters calculated by linear regression for different Pb(II) initial concentrations are summarized in Table 4. Plots of pseudo-first-order and pseudo-second-order kinetic and intra-particle diffusion models are shown in Figs. 5(a) through (c) for the effect of initial Pb(II) concentrations. As shown in Table 4, the coefficients of determination (R^2) obtained from the plots of pseudo second-order kinetics were larger ($R^2 > 0.999$) than those of the pseudo-first-order and intra-particle diffusion models for all studied initial Pb(II) concentration. Furthermore, the values of SD obtained from the pseudo-second-order model were much lower than that of the other kinetic models.

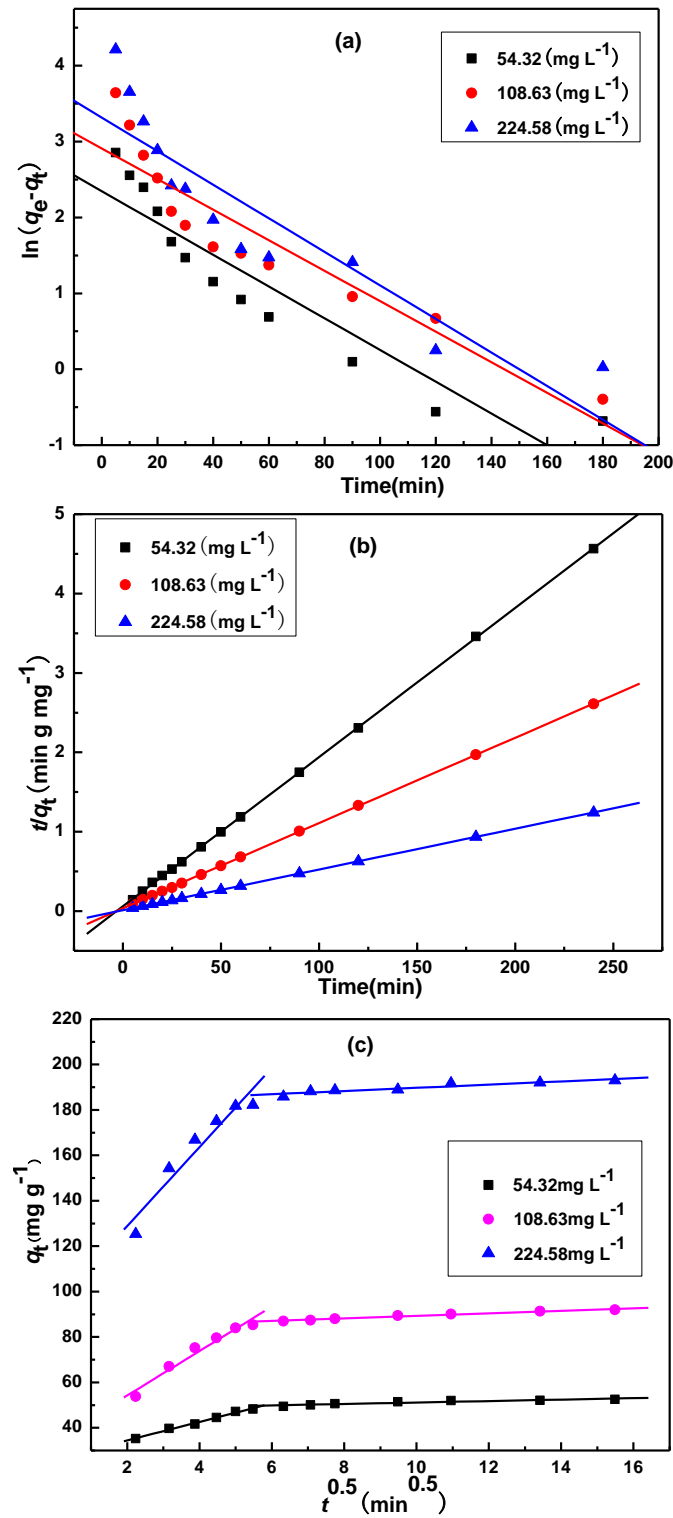


Fig. 5. Kinetic plots for adsorption of Pb (II) onto sesame leaf: (a) pseudo first-order; (b) pseudo second-order; and (c) intraparticle diffusion at different initial Pb (II) concentrations (T = 303 K; C_{dosage}=1g L⁻¹; initial pH 5.0)

Table 4. Kinetic Parameters of Different Kinetic Models (T=303 K, initial pH 5.0, $C_{\text{dosage}} = 1.0 \text{ g L}^{-1}$)

C_0 (mg L ⁻¹)	54.32	108.63	224.58
Pseudo-first order			
$q_{e, \text{exp}}$ (mg g ⁻¹)	52.30	92.00	193.89
$q_{e, \text{calc}}$ (mg g ⁻¹)	10.45	18.33	27.60
k_1 (min ⁻¹) × 10 ²	2.09	2.01	2.21
R^2	0.8657	0.8644	0.8253
SD	0.453	0.438	0.560
Pseudo-second order			
$q_{e, \text{calc}}$ (mg g ⁻¹)	53.22	93.11	194.93
h_0 (mg g ⁻¹ min ⁻¹)	16.12	27.58	87.03
k_2 (g mg ⁻¹ min ⁻¹) × 10 ³	5.69	3.18	2.29
R^2	0.9999	0.9999	0.9999
$SD \times 10^3$	9.33	5.06	2.02
Intraparticle diffusion			
k_{d1} (mg g ⁻¹ min ^{-1/2})	4.07	9.79	17.41
C_1 (mg g ⁻¹)	26.31	34.64	93.98
R^2	0.9917	0.9626	0.9255
SD	0.50	2.59	6.64
$k_{d,2}$ (mg g ⁻¹ min ^{-1/2})	0.32	0.56	0.71
C_2 (mg g ⁻¹)	47.93	83.68	182.68
R^2	0.8731	0.9789	0.8850
SD	0.46	0.31	0.95

The value of SD relates to the conformity between the experimental data and the model-predicted values. In general, the lower the SD , the greater is the conformity effect. On the other hand, the calculated values of $q_{e, \text{cal}}$ obtained from the pseudo-second-order model perfectly agreed with the experimental values of $q_{e, \text{exp}}$ at three initial concentrations. These results revealed that the pseudo-second-order model was the best

one in describing the kinetics of Pb(II) adsorbed onto sesame leaf powder. According to the pseudo-second-order model, boundary layer resistance was not the rate-limiting step, the external resistance model cannot sufficiently explain the adsorption mechanism, and the rate-limiting step might be chemical adsorption involving valence forces by sharing of electrons between anions and biosorbent (Al-Ghouthi *et al.* 2005).

It can also be seen in Table 4 that, with an increase in initial metal concentration, the initial adsorption rate (h_0) increased from 16.12 to 87.07 mg g⁻¹ as the initial concentration increased from 50 to 300 mg L⁻¹. This may be attributed to the increase of driving force between the liquid and solid phase with the increasing Pb(II) concentration. On the other hand, the rate constant (k_2) of pseudo second-order presented the opposite trend. A similar observation has been also reported by earlier researchers (Papandreou *et al.* 2007; Allen *et al.* 2005).

As shown in Fig. 5c, none of the lines passed through the origin. This indicates that the intra-particle diffusion was not the only rate-controlling step (Khaled *et al.* 2009). Other mechanisms such as boundary layer may dominate the adsorption process to some extent (Qin *et al.* 2009). The values of k_d and C obtained from the linear regression analysis were listed in Table 4. It was observed that with the increasing initial Pb(II) concentration from 54.32 to 224.58 mg L⁻¹, the values of C increased from 26.31 to 93.98 mg g⁻¹ and from 47.93 to 182.68 mg g⁻¹ in the two stages, respectively, which reflected the increase in the thickness of boundary layer (Wang *et al.* 2010), and the decrease in the chance of external mass transfer. Hence the chance of internal mass transfer was increased (Khaled *et al.* 2009).

CONCLUSIONS

1. The adsorption of lead ions from aqueous solution using the agricultural by-product sesame leaf was investigated. Various impact factors such as contact time, initial lead ions concentration, solution pH, and adsorbent dosage were optimized.
2. The sorption data fitted both the Langmuir and Koble–Corrigan isotherms with high R^2 and low χ^2 values. The monolayer saturation adsorption capacities of sesame leaf for lead ions were 279.86, 283.01, and 298.76 mg g⁻¹ at different temperatures 293, 303, and 313 K, respectively. A negative value of ΔG^0 and positive value of ΔH^0 confirmed the spontaneous and endothermic nature of the adsorption process.
3. The kinetic studies indicated that the pseudo second-order model was the best one in describing the kinetics of Pb(II) adsorbed onto sesame leaf powder. In addition, the intraparticle diffusion of lead ions into micropores was not the sole rate-controlling step.
4. A large number of carbonyl and hydroxyl groups were observed on the surface of the material by FTIR analysis.

REFERENCES CITED

- Afridi, H. I., Kazi, T. G., Kazi, G. H., Jamali, M. K., and Shar, G. Q. (2006). "Essential trace and toxic element distribution in the scalp hair of Pakistani myocardial infarction patients and controls," *Biol. Trace Elem. Res.* 113(1), 19-34.
- Al-Ghouti, M., Khraisheh, M. A. M., Ahmad, M. N. M., and Allen, S. (2005). "Thermodynamic behavior and the effect of temperature on the removal of dyes from aqueous solution using modified diatomite: a kinetic study," *J. Colloid Interf. Sci.* 287(1), 6-13.
- Allen, S. J., Gan, Q., Matthews, R., and Johnson, P. A. (2005). "Kinetic modeling of the adsorption of basic dyes by kudzu," *J. Colloid Interf. Sci.* 286 (1), 101-109.
- Allouch, F. N., Mameri, N., and Guibal, E. (2011). "Pb(II) biosorption on *Posidonia oceanica* biomass," *Chem. Eng. J.* 168 (1), 1174-1184.
- Amarasinghe, B. M. W. P. K., and Williams, R. A. (2007). "Tea waste as a low cost adsorbent for the removal of Cu and Pb from wastewater," *Chem. Eng. J.* 132(1-3), 299-309.
- Astier, C., Chaleix, V., Faugeron, C., Ropartz, D., Krausz, P., and Gloaguen, V. (2012). "Biosorption of lead(II) on modified barks explained by the hard and soft acids and bases (HSAB) theory," *BioResources* 7(1), 1100-1110.
- Axtell, N. R., Sternberg, S. P. K., and Claussen, K. (2003). "Lead and nickel removal using microspora and *lemna minor*," *Bioresource Technol.* 89(1), 41-48.
- Bulut, Y., and Baysal, Z. (2006). "Removal of Pb(II) from wastewater using wheat bran," *J. Environ. Manage.* 78(2), 107-113.
- Chen, H., and Wang, A. Q. (2009). "Adsorption characteristics of Cu(II) from aqueous solution onto poly(acrylamide)-attapulgit composite," *J. Hazard. Mater.* 165(1-3), 223-231.
- Chen, H., Zhao, J., Dai, G. L., Wu, J. Y., and Yan, H. (2010). "Adsorption characteristics of Pb(II) from aqueous solution onto a natural biosorbent, fallen *Cinnamomum camphora* leaves," *Desalination* 262(1-3), 174-182.
- Cruz-Olivares, J., Perez-Alonso, C., Barrera-Diaz, C., Lopez, G., and Balderas-Hernandez, P. (2010). "Inside the removal of lead(II) from aqueous solutions by de-oiled allspice husk in batch and continuous processes," *J. Hazard. Mater.* 181(1-3), 1095-1101.
- dos Santos, W. N. L., Cavalcante, D. D., da Silva, E. G. P., das Virgens, C. F., and Dias, F. D. (2011). "Biosorption of Pb(II) and Cd(II) ions by *Agave sisalana* (sisal fiber)," *Microchem. J.* 97(2), 269-273.
- Foo, K. Y., and Hameed, B. H. (2010). "Insights into the modeling of adsorption isotherm systems," *Chem. Eng. J.* 156 (1), 2-10.
- Freundlich, H. M. F. (1906). "Über die Adsorption in Lösungen," *J. Phys. Chem.* 57, 385-470.
- García-Rosales, G., Olguin, M. T., Colín-Cruz, A., and Romero-Guzmán, E. T. (2012). "Effect of the pH and temperature on the biosorption of lead(II) and cadmium(II) by sodium-modified stalk sponge of *Zea mays*," *Environ. Sci. Pollut. Res.* 19(1), 177-185.
- Gupta, V. K., and Rastogi, A. (2008). "Biosorption of lead from aqueous solutions by

- green algae *Spirogyra* species: Kinetics and equilibrium studies,” *J. Hazard. Mater.* 152(1), 407-414.
- Han, R. P., Zhang, L. J., Song, C., Zhang, M. M., Zhu, H. M., and Zhang, L. J. (2010). “Characterization of modified wheat straw, kinetic and equilibrium study about copper ion and methylene blue adsorption in batch mode,” *Carbohydr. Polym.* 79(4), 1140-1149.
- Haron, M. J., Tiansin, M., Ibrahim, N. A., Kassim, A., Yunus, W. M. Z. W., and Talebi, S. M. (2011). “Sorption of Pb(II) by poly(hydroxamic acid) grafted oil palm empty fruit bunch,” *Water Sci. Technol.* 63(8), 1788-1793.
- Iqbal, M., Saeed, A., and Zafar, S. I. (2009). “FTIR spectrophotometry, kinetics and adsorption isotherms modeling, ion exchange, and EDX analysis for understanding the mechanism of Cd²⁺ and Pb²⁺ removal by mango peel waste,” *J. Hazard. Mater.* 164(1), 161-171.
- Javed, M. A., Bhatti, H. N., Hanif, M. A., and Nadeem, R. (2007). “Kinetic and equilibrium modeling of Pb(II) and Co(II) sorption onto rose waste biomass,” *Separ. Sci. Technol.* 42(16), 3641-3656.
- Jayaramudu, J., Maity, A., Sadiku, E.R., Guduri, B.R., Varada Rajulu, A., Ramana, CH. V. V., and Li, R. (2011). “Structure and properties of new natural cellulose fabrics from *Cordia dichotoma*,” *Carbohydr. Polym.* 86(4), 1623-1629.
- Kavitha, D., and Namasivayam, C. (2007). “Experimental and kinetic studies on methylene blue adsorption by coir pith carbon,” *Bioresour. Technol.* 98 (1), 14-21.
- Kazi, T. G., Jalbani, N., Kazi, N., Jamali, M. K., Arain, M. B., Afridi, H. I., Kandhro, A., and Pirzado, Z. (2008). “Evaluation of toxic metals in blood and urine samples of chronic renal failure patients, before and after dialyses,” *Renal Failure* 30(7), 737-745.
- Khaled, A., El Nemr, A., El-Sikaily, A., and Abdelwahab, O. (2009). “Removal of Direct N Blue-106 from artificial textile dye effluent using activated carbon from orange peel: Adsorption isotherm and kinetic studies,” *J. Hazard. Mater.* 165(1-3), 100-110.
- Kul, AR., and Koyuncu, H. (2010). “Adsorption of Pb(II) ions from aqueous solution by native and activated bentonite: Kinetic, equilibrium and thermodynamic study,” *J. Hazard. Mater.* 179(1-3), 332-339.
- Langmuir, I. (1916). “The constitution and fundamental properties of solids and liquids,” *J. Am. Chem. Soc.* 38, 2221-2295.
- Liu, Y. W., Chang, X. J., Guo, Y., and Meng, S. M. (2006). “Biosorption and preconcentration of lead and cadmium on waste Chinese herb Pang Da Hai,” *J. Hazard. Mater.* 135(1-3), 389-394.
- Martinez, M., Miralles, N., Hidalgo, S., Fiol, N., Villaescusa, I., and Poch, J. (2006) “Removal of lead (II) and cadmium (II) from aqueous solutions using grape stalk waste,” *J. Hazard. Mater.* 133(1-3), 203-211.
- Martins, R. J. E., and Boaventura, R. A. R. (2011). “Modelling of lead removal by an aquatic moss,” *Water Sci. Technol.* 63(1), 136-142.
- Mihailescu Amalinei, R. L., Miron, A., Volf, I., Paduraru, C., and Tofan, L. (2012). “Investigations on the feasibility of Romanian pine bark wastes conversion into a value-added sorbent for Cu(II) and Zn(II) ions,” *BioResources* 7(1), 148-160.

- Mudhoo, A., Garg, V. K., and Wang, S. B. (2011). "Removal of heavy metals by biosorption," *Environ. Chem. Lett.* DOI 10.1007/s10311-011-0342-2.
- Ngah, W. S. W., and Hanafiah, M. A. K. M. (2008). "Biosorption of copper ions from dilute aqueous solutions on base treated rubber (*Hevea brasiliensis*) leaves powder: kinetics, isotherm, and biosorption mechanisms," *J. Environ. Sci-China.* 20 (10), 1168-1176.
- Ozcan, AS., Tunali, S., Akar, T., and Ozcan, A. (2009). "Biosorption of lead (II) ions onto waste biomass of *Phaseolus vulgaris* L.: Estimation of the equilibrium, kinetic and thermodynamic parameters," *Desalination* 244 (1-3), 188-198.
- Papandreou, A., Stournaras, C. J., and Panias, D. (2007). "Copper and cadmium adsorption on pellets made from fired coal fly ash," *J. Hazard. Mater.* 148(3), 538-547.
- Qaiser, S., Saleemi, A. R., and Umar, M. (2009). "Biosorption of lead from aqueous solution by *Ficus religiosa* leaves: Batch and column study," *J. Hazard. Mater.* 166 (2-3), 998-1005.
- Qin, Q. D., Ma, J., and Liu, K. (2009). "Adsorption of anionic dyes on ammonium-functionalized MCM-41," *J. Hazard. Mater.* 162(1), 133-139.
- Saeed, A., Iqbal, M., and Akhtar, M. W. (2005). "Removal and recovery of lead(II) from single and multi-metal (Cd, Cu, Ni, Zn) solutions by crop milling waste (black gram husk)," *J. Hazard. Mater.* 117 (1), 65-73.
- Saka, C., Sahin, O., Demir, H., and Kahyaoglu, M. (2011). "Removal of lead(II) from aqueous solutions using pre-boiled and formaldehyde-treated onion skins as a new adsorbent," *Separ. Sci. Technol.* 46(3), 507-517.
- Sari, A., Tuzen, M., Citak, D., and Soylak, M. (2007). "Adsorption characteristics of Cu(II) and Pb(II) onto expanded perlite from aqueous solution," *J. Hazard. Mater.* 148(1-2), 387-394.
- Singh, N., and Gadi, R. (2012). "Studies on biosorption of Pb (II) by the nonliving biomasses of *Pseudomonas oleovorans* and *Brevundimonas vesicularis* and its removal from wastewater samples," *Eur. J. Scientific Res.* 69(2), 279-289.
- Vimala, R., and Das, N. (2009). "Biosorption of cadmium (II) and lead (II) from aqueous solutions using mushrooms: A comparative study," *J. Hazard. Mater.* 168(1), 376-382.
- Wang, L., Zhang, J., Zhao, R., Li, Y., Li, C., and Zhang, C. L. (2010). "Adsorption of Pb(II) on activated carbon prepared from *Polygonum orientale* Linn.: Kinetics, isotherms, pH, and ionic strength studies," *Bioresource Technol.* 101(15), 5808-5814.
- Weber Jr., W. J., and Morris, J. C. (1963). "Kinetics of adsorption on carbon from solution," *J. Sanit. Eng. Div. Proceed. Am. Soc. Civil Eng.* 89, 31-39.
- Webi, T. W., and Chakravort, R. K. (1974). "Pore and solid diffusion models for fixed-bed adsorbers," *AIChE J.* 20(2), 228-238.
- Weng, C. H. (2004). "Modeling Pb(II) adsorption onto sandy loam soil," *J. Colloid Interf. Sci.* 272(2), 262-270.

Article submitted: April 8, 2012; Peer review completed: June 2, 2012; Revised version received: June 17, 2012; Accepted: June 18, 2012; Published: June 21, 2012.